

# Evolution of HTS rf SQUIDS

Yi Zhang

**Abstract**—I present the evolution of rf-SQUIDS towards modern planar thin film devices. My main objective is to describe our own planar HTS rf washer SQUIDS and their operation with coplanar resonators and multiturn flux transformers. This publication is dedicated to the memory of J.E. Zimmerman, whose ideas have guided us through the development of rf SQUID planar technology.

## I. INTRODUCTION

Jim Zimmerman contributed not only to the development of bulk superconducting quantum interference devices (SQUIDS) from conventional materials (LTS) [1], [2], but he also was the first to demonstrate high-temperature superconductor (HTS) radio-frequency (rf) SQUIDS with break junctions [3]. While he did not develop thin film SQUIDS, his ideas had a great impact on the development of planarized structures. For example, his fractional turn SQUID idea was later implemented in thin-film, low-inductance dc SQUIDS [4]–[6].

In the early 80's, Jaycox and Ketchen introduced the washer SQUID in order to achieve a tight coupling between the SQUID loop and an integrated input coil [7]. This, and the reliable Nb/Al<sub>2</sub>O<sub>3</sub> junction technology, greatly improved the performance, reproducibility and applicability of dc SQUID magnetometers. Commercial multi-channel systems, e.g. for magnetoencephalography, thus became possible [8], [9].

In fact, the availability of high-performance dc SQUIDS removed the incentive to develop thin-film rf SQUIDS which were believed to be less sensitive. Only the advent of HTS provided that incentive. In this publication, we review the challenges of developing low-noise HTS thin film rf SQUIDS and show specific solutions which make their performance comparable to that of dc SQUIDS.

## II. FIRST GENERATION HTS RF SQUID MAGNETOMETERS

Sensitive HTS magnetometers can only be made as planar structures, due to the absence of thin HTS wires for use as pickup coils.

All our superconducting structures discussed below were patterned from 200 nm thick epitaxial YBa<sub>2</sub>Cu<sub>3</sub>O<sub>7</sub> (YBCO) films, typically on 1 mm thick LaAlO<sub>3</sub> substrates. We fabricated the rf SQUIDS using step-edge junctions [10]. The need for only one junction in rf SQUID was seen as a potential advantage in the early stages of HTS technology. An overview of past and recent work on junction technologies and HTS rf SQUIDS can be found elsewhere [11]–[13].

The field resolution  $B_N$  of a magnetometer is determined by two factors:

$$B_N = \frac{\partial B}{\partial \phi} \times S_\phi^{1/2},$$

where  $\partial B/\partial \phi$  is the flux-to-field transformation coefficient and  $\sqrt{S_\phi}$  is the flux noise of the SQUID. Larger washers lead to smaller values of the flux-to-field coefficient and thus improve the field resolution.

Our first successful design for HTS rf SQUID magnetometers comprised a large washer area of about  $8 \times 8 \text{ mm}^2$  used as a flux focusing structure (see Fig. 1). In 1992, we could demonstrate a field resolution,  $B_N$ , of less than 200 fT/ $\sqrt{\text{Hz}}$  at 77 K. With such washer SQUIDS, we could not only measure the human heart signal but were also able to detect an auditory evoked brain signal in a standard magnetically shielded room [14], [15].

The effective area of the SQUID washer — and thus its field resolution — can be increased by the use of further flux concentrators in a flip-chip configuration. For example, concentrators from bulk material or thin films of 1" in diameter reduce the field-to-flux coefficient from about 2 to 0.6 nT/ $\phi_0$ . Using this approach, Tavrín and Borgmann assembled first- and second-order gradiometers and detected human heart signals in a magnetically unshielded environment [16], [17].

In this first generation of HTS rf SQUID magnetometers:

- The conventional tank circuit consisted of lumped elements like in bulk technology. The rf-bias frequency was lower than 300 MHz.
- The SQUID magnetometer comprised a single-layer or flip-chip washer with a large area. The flux noise of the SQUIDS was relatively high,  $\sqrt{S_\phi} = 60$  to  $100 \mu\phi_0/\sqrt{\text{Hz}}$  for SQUID inductances  $L_S$  of about 150 to 300 pH.

The success of this generation of HTS rf SQUID magnetometers is due to the reduction of the value of the flux-to-field coefficient by the large washer area. However, the flux noise of the SQUID system still remained large. Solution to this problem was found in the second generation of HTS rf SQUID magnetometers.



Fig. 1. Schematic layout of a large washer rf SQUID. The Josephson junction is located between the SQUID loop in the centre and the slit.

Manuscript received September 18, 2000.  
Institut für Schicht- und Ionentechnik, Forschungszentrum Jülich, 52425 Jülich, Germany (email: y.zhang@fz-juelich.de; ph: +49-2461-61-2691).

### III. SECOND GENERATION HTS RF SQUID MAGNETOMETERS

#### A. Considerations for Optimum Tank Circuit Behavior

Kurkijärvi developed a theory of noise in rf-SQUID systems [18], and identified three sources of noise:

- intrinsic noise in the SQUID
- noise of the tank circuit (and connecting cable)
- preamplifier noise.

According to this theory, the increase of the rf-bias frequency  $f_0$  reduces the system flux noise.

Subsequently, Jackel and Buhrman [19] and others experimentally verified this theory. We note here that this theory is based on the assumption of a high impedance of the tank circuit and, especially, of the preamplifier. In practice, the cable between the tank circuit and the preamplifier forms part of the tank circuit, and thus puts an upper limit on  $f_0$ . Also, the preamplifier cannot maintain a high input impedance at high frequencies. Using the scheme of a high impedance,  $f_0$  usually was lower than 40 MHz. The loaded quality factor  $Q$  of the lumped element tank circuit was in the range of several tens at 77 K.

To further increase  $f_0$ , several low-impedance connection schemes using 50  $\Omega$  cables between the tank circuit and the preamplifier were developed [20]-[22]. One of them was used for the first generation of HTS SQUID magnetometers.

An ideal tank circuit fulfils the following requirements:

- high rf-bias frequency  $f_0$
- high unloaded quality factor  $Q_0$
- proper coupling  $k^2$  between the tank circuit and the SQUID loop ( $k^2Q > 1$  must be fulfilled [23], [24])
- easy adjustment of the impedance matching between the tank circuit and the connecting cable.

#### B. Planar Resonators Serving as Tank Circuits

Several resonators were investigated and evaluated for optimum operation with thin film rf SQUIDs

##### a) The $\lambda/2$ -Resonator

Mück and Heiden were the first to introduce planar superconducting tank circuits for operation of LTS rf SQUIDs [25]. A microstrip line made from niobium thin film served as a resonator, evaporated onto a sapphire substrate. The  $f_0$  of this resonator corresponds to its effective half wavelength,  $\lambda$ . This  $\lambda/2$ -resonator structure consisted of the microstrip line, the substrate as a dielectric and a metallic ground plane.



Fig. 2. Schematic layout of rf SQUID integrated with a  $\lambda/2$ -resonator.

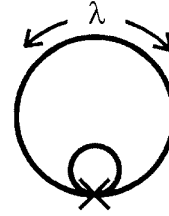


Fig. 3. Equivalent circuit of the SQUID integrated with the  $\lambda$ -resonator. The large ring acts as resonator and as pickup loop. The small ring represents the SQUID loop.

The maximum voltages of the resonator are located at the resonator ends, while the maximum current is at the center. The SQUID was patterned at this very location (see Fig. 2) to enhance its coupling to the resonator, so that  $k^2Q > 1$  could be satisfied.

In these experiments, the  $\lambda/2$ -resonator had a resonant frequency of about 3 GHz. Because of the employment of a superconducting resonator, the flux noise,  $\sqrt{S_\phi}$ , of the rf SQUID system was reduced to values thus far known only for LTS dc SQUIDs. Using HTS thin films we, too, could obtain low  $\sqrt{S_\phi}$  with an S-shaped 3 GHz microstrip resonator [26].

The work by Mück and Heiden was the first successful demonstration of a thin film rf SQUID system with flux noise as low as in the best dc SQUIDs. They also were the first to integrate the resonator with the SQUID on a single substrate.

Unfortunately, the use of the microstrip line as both the tank circuit and the flux concentrator wasn't ideal for single-layer HTS magnetometers, because it produced too low of an effective area (high  $\partial B/\partial \phi$ ). Ideally, the entire area of the substrate could be used to concentrate flux, as in the first generation magnetometers, but optimum operation for rf SQUIDs must be fulfilled to attain low flux noise.

##### b) The $\lambda$ -Resonator and Two Other Resonators

A closed microstrip line (ring) can be used as a full-wavelength ( $\lambda$ )-resonator. This ring can also act as a pick-up loop for the SQUID magnetometer [27]. A schematic of this layout is shown in Fig. 3. This concept seemed very promising for magnetometer layouts, but the coupling between the SQUID and the resonator was found to be too small ( $k^2Q < 1$ ), although the  $Q$  value can be rather large. From these investigations, we learned that the coupling is largely determined by the current distribution in the resonator, and a high  $Q$  value alone is not a sufficient criterion for proper SQUID operation. Subsequently, we experimented with bulk dielectric resonators [28] and planar lumped element (hairpin) resonators [29].

All of these permitted us to obtain a high resonant frequency, a high unloaded quality factor  $Q_0$ , and an improved flux focusing. However, for different reasons, none of them was practical for optimum operation. The  $k^2Q$  was either too low or too difficult to adjust. Nevertheless, some of these approaches might still have potential for the future.

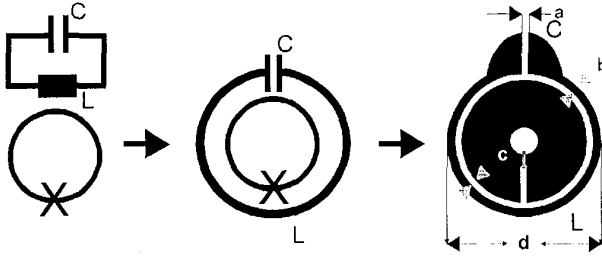


Fig. 4. Evolution of our resonator structures. Conventional tank circuit with SQUID (left), schematic representation of rf SQUID with planar resonator (middle), integrated design with rf SQUID washer surrounded by a resonator (right).

#### c) Washer SQUIDs with Surrounding Planar Resonators

In the process of our investigations, an evolution of the resonator structure has taken place. In bulk HTS SQUIDs the coil of the tank circuit is located inside the SQUID loop. In our planar layout [30], however, we settled on the tank circuit resonator surrounding the large SQUID washer, as shown in Fig. 4. A microstrip line (or a modified planar hairpin resonator) is integrated with a large washer on a single chip. The coupling is not galvanic, like in the case of the  $\lambda/2$ - and  $\lambda$ -resonator, but inductive, like in the case of bulk SQUIDs.

We found four advantages of such planar resonators:

- A optimum combination of superconducting planar resonator and large area washer SQUID could be obtained on a single substrate.
- The inductive coupling coefficient  $k$  between the SQUID and the resonator could be estimated easily from simple geometrical considerations. A more accurate value of this coefficient could be simulated by taking the actual current density in the structure into account [31].
- We could use inductive coupling to easily match the electronics to the SQUID. The matching loop, shown in Fig. 5, can also be employed for flux modulation and as feedback coil. Thus, the SQUID system could be operated by a single cable in contrast to the earlier capacitive matching solution, which required another cable for flux modulation and feedback [25].
- The requirement  $k^2Q > 1$  could be easily fulfilled. The flux noise was reduced by this scheme, such that—for the first time—the white noise level of HTS rf-SQUIDs was comparable to that of dc-SQUIDs. Already in preliminary experiments in open loop configuration, we obtained a white flux noise of  $\sqrt{S_\phi} \approx 20 \mu\phi_0/\sqrt{\text{Hz}}$  at  $L_S = 150 \text{ pH}$ , resulting in a field resolution of  $B_N = 50 \text{ fT}/\sqrt{\text{Hz}}$  for a  $1 \text{ cm}^2$  chip. For  $L_S = 50 \text{ pH}$ , we obtained  $8 \mu\phi_0/\sqrt{\text{Hz}}$ .

#### d) SQUIDs with Coplanar Resonators

All of the resonators described above required a metallic ground plane. At the level of  $B_N = 50 \text{ fT}/\sqrt{\text{Hz}}$ , the thermally activated field noise from a normal conducting ground plane dominates the system noise below about 10 kHz [32].

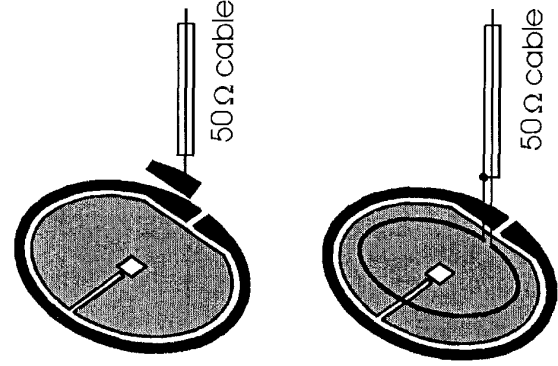


Fig. 5. Two matching schemes between the resonator and the readout electronics. Capacitive coupling on the left, inductive coupling on the right.

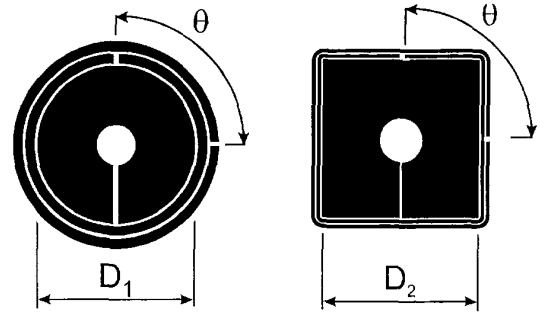


Fig. 6. Schematic of two flux concentrator/coplanar resonator layouts. A rf washer SQUID, 2.5 or 3.5 mm in diameter, is placed onto the concentrator to form a flip-chip package.

Since we didn't want to use a superconducting ground plane on a separate substrate, we eventually settled on a coplanar resonator, to simply get rid of the ground plane [33],[34].

Figure 6 shows two examples of the integration of circular and square coplanar resonator with the flux concentrator. The inner hole of the concentrator was 1.5 mm in diameter. The SQUID is positioned (centered) on top of the concentrator. We adopted the flip-chip configuration as standard, to be able to fabricate on one substrate multiple small SQUIDs, 2.5 to 3.5 mm in diameter, and thus to improve fabrication yield.

The width of the two coplanar microstrip lines was 100-200  $\mu\text{m}$  each, while radial spacings between the concentrator and the inner microstrip line and between the microstrip lines themselves were about 100  $\mu\text{m}$ .

We varied the angle  $\theta$  between two microstrip resonator slits openings, to adjust the resonant frequency. The introduction of a short between microstrip lines offered another possibility to adjust  $f_0$  over an even wider range. The angular position of this optional short relative to the opening of the inner microstrip is denoted by  $\xi$ .

Table 1 shows the dependence of the resonant frequency on layout parameters, such as the diameter of the resonator, the angle  $\theta$ , and the short position  $\xi$ . Details are given in [34]. Table 2 shows the best recorded values of white noise spectral density, and the corresponding  $B_N$  values.

TABLE I  
DEPENDENCE OF THE RESONATOR FREQUENCY ON THE LAYOUT  
PARAMETERS

$D_1, D_2^*$ [mm]	$\theta$ [deg]	$\xi$ [deg]	$f_0$ [MHz]
8.1	90	-	1170
8.1	90	-90	961
8.5*	0	-	1190
8.5*	90	-	910
8.5*	90	-90	740
8.5*	180	-	815
8.5*	180	-90	550
13.4	0	-	790
13.4	90	-	630
13.4	180	-	590

$D_1, D_2$  denote the sizes of the concentrator washer in Fig. 6 in the case of the circular and the square layout. Where no value for  $\xi$  is specified, the layout does not feature a shorting connection between the two microstrips.

TABLE II  
PERFORMANCE DATA OF SQUIDS WITH COPLANAR RESONATORS

$D_1, D_2^*$ [mm]	$f_0$ [MHz]	LOOP SIZE [ $\mu\text{m}^2$ ]	$\partial B/\partial \phi$ [nT/ $\phi_0$ ]	$\sqrt{S_\phi}$ [ $\mu\phi_0/\sqrt{\text{Hz}}$ ]	$B_N$ [fT/ $\sqrt{\text{Hz}}$ ]
8.1	1100	100×100	4.7	8.3	40
8.5*	910	100×100	3.9	6.5	26
8.5*	810	10×500	2.55	9	23
8.5*	810	15×500	2.4	14.4	35
13.4	650	10×500	1.85	8.5	16
13.4	635	50×500	1.23	16	20
13.4	630	100×100	3.1	7.5	23

Values of flux noise and field resolution were obtained in white noise region.

By using coplanar resonators, we could further reduce the flux noise. The best white noise value measured so far for a SQUID inductance of 260 pH was about  $8.5 \mu\phi_0/\sqrt{\text{Hz}}$ . This is only a factor of 3 above the thermal noise  $L_s \times (4k_B T/R_N)^{1/2}$ , assuming a typical value of  $9 \Omega$  for the normal resistance  $R_N$  of the junction [35],  $k_B$  being Boltzmann's constant. This noise level corresponds to an uncoupled energy resolution of about  $5.6 \times 10^{-31} \text{ J/Hz}$  or about 850 h, where  $h$  is Planck's constant.

Traditionally, rf SQUIDs operated at a low rf-bias frequency, and cooled by liquid helium, had energy resolution only slightly better than  $\epsilon_E = 1 \times 10^{-29} \text{ J/Hz}$ , yet our experimental values at 77K are over an order of magnitude lower. Our low- $\epsilon_E$  SQUIDs operate in the dispersive regime. These results are in semi-quantitative agreement with an extension of the conventional rf SQUID theory by Chesca [36], which was experimentally verified for our SQUIDs by Zeng et al. [35]. In the optimum regime, the flux-voltage characteristics of the rf SQUID is not triangular, but has a nearly rectangular form with large  $\partial V/\partial \phi$ -values in the range of several  $100 \mu\text{V}/\phi_0$ . Thus, the preamplifier contributes less to the system noise.

### C. Planar "Toroidal" Layout

Interestingly, low-frequency flux noise in SQUIDs with a coplanar resonator is not reduced in comparison to the conventional tank circuit (for example, see Fig. 2 of [33]).

There are only a few publications on the low-frequency behavior of rf SQUIDs. Mück et al. discussed the low frequency noise caused by fluctuations of the junction resistance and critical current [37]. We have described the low frequency noise caused by bubbling of liquid nitrogen [38]. Yet neither mechanism seems to cause the observed low frequency noise in our coplanar resonator SQUID.

The bias point of dc SQUIDs is determined by the applied bias current,  $I_b$ . The environment has practically no influence on the value of  $I_b$ , as long as the SQUID is not shunted by an external parallel resistor. For rf SQUIDs, however, metallic or dielectric objects brought in close vicinity to the SQUID or the tank circuit can change the rf field distribution between the SQUID and the tank circuit and thus its operating point, even if these objects are nonmagnetic. As a consequence, additional low-frequency noise can be introduced by these processes.

In our coplanar layout, the resonator surrounds the washer and radiates into space, i.e., this configuration is an open system with the surroundings being part of the resonator. To enhance the stability of the SQUID operating point, the electromagnetic field radiated by the resonator has to be confined to the vicinity of the SQUID.

This can be achieved by two methods. First, the  $\text{LaAlO}_3$  substrate can be replaced by  $\text{SrTiO}_3$ , whose dielectric constant  $\epsilon$  is two orders of magnitude higher and thus confines the rf energy of the resonator mostly inside the substrate. Second, the coplanar resonator can be embedded into the washer (pickup loop) as shown in Fig. 7. In this case, the pickup loop, apart from concentrating the magnetic flux into the SQUID, shields the resonator and thus reduces (limits) its radiation.

In bulk technology, this idea was implemented already in 1973 as the, so-called, toroidal SQUID [39] [40]. At that time, the excellent coupling between the SQUID and the tank circuit, and the excellent shielding against external magnetic disturbances had been mentioned. Here, we point out that the stabilization of the rf SQUID operating point is another advantage of the toroidal structure.

In the layout of Fig. 7 on  $1 \text{ cm}^2$  substrates, we obtained  $f_0$  values of about 500 MHz and  $Q_0$  values of several 1000 at 77 K. First noise measurements showed a field noise of about 50 fT/ $\sqrt{\text{Hz}}$  at less than 5 Hz. Details of this work will be reported in a future publication.

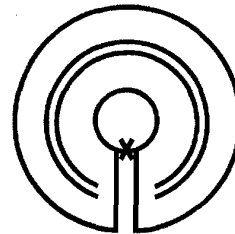


Fig. 7. Equivalent circuit of the planar toroidal SQUID. The coplanar resonator is located between the SQUID loop (center), and the pickup loop (circumference).

#### D. Second Generation rf SQUID magnetometers: Summary

The development of the second generation of HTS rf SQUID magnetometers took about 8 years. The goal of the second generation, the reduction of the flux noise, was achieved by the integration of the large washer SQUID with the coplanar resonator. Such resonators may comprise more than two microstrip lines. This leads to the labyrinth resonators described next.

Using the described 2<sup>nd</sup> generation SQUIDs we demonstrated many SQUID applications in biomagnetism, geomagnetism and nondestructive evaluation [41]-[43].

The field resolution may further be enhanced by the use of a multiturn flux transformer, which improves the value of  $\partial B/\partial \phi$ .

#### IV. THIRD GENERATION HTS RF SQUID MAGNETOMETERS

The improvement of field sensitivity of HTS dc SQUID magnetometers by planar multiturn flux transformers has been demonstrated [44], [45]. However, rf SQUID magnetometer had never been used in combination with a planar multilayer structure.

At first, we replaced the flux concentrator by a multiturn flux transformer. Its pickup loop was surrounded by the coplanar resonator. However, the resonance of the resonator could no longer be observed, once the connecting strip (crossover) was closed, due to damping [46]. This behaviour was also confirmed by computer simulations [47].

We eventually understood that the rf circuit must be separated from the dc circuit (here, the flux transformer consisting of a pickup loop and an input coil is called "dc circuit".)

In [46], we describe our solution, a planar double-hole SQUID that is coupled to a pickup loop with two input coils in flip-chip configuration. This was the first successful design of a multi-

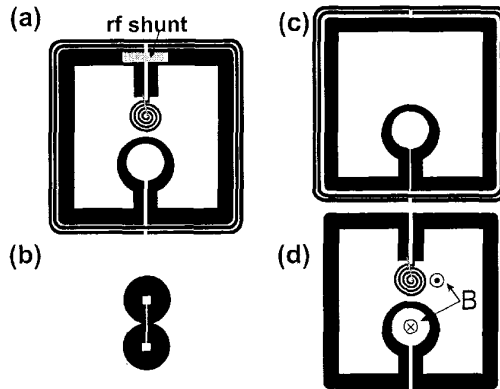


Fig. 8 Layouts and equivalent circuits of a planar rf SQUID magnetometer. (a) A coplanar resonator integrated with a flux transformer with a metal strip shunting the multi-turn input coil. (b) A double-hole washer SQUID. (c) Equivalent circuit for rf currents. (d) Equivalent circuit for dc currents.

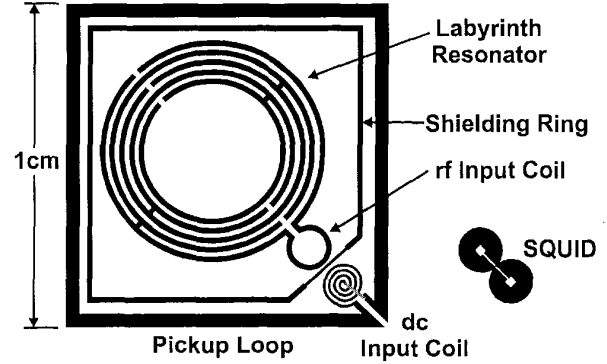


Fig. 9. Layout of the rf SQUID magnetometer with labyrinth resonator. The SQUID is positioned on the two input coils in flip-chip configuration.

layer transformer for rf SQUID operation. Fig. 8a shows the layout of this SQUID magnetometer. The coplanar resonator surrounds the pickup loop. A thin-film normal metal shunt is introduced to short the multiturn transformer coil, resulting, for high frequencies, in an equivalent circuit of Fig. 8c. For low frequencies, however, this shunt has no effect because of the superconducting input coil, which leads to an equivalent circuit shown in Fig. 8d. A double-hole SQUID of Fig. 8b is placed onto the resonator chip in the flip-chip configuration.

This design was inspired by the double-hole SQUID of Zimmerman et al [2]. In the niobium bulk technology, they separated the rf and the dc circuits. One hole of a double-hole SQUID was coupled to the dc circuit, the other one to the rf circuit (tank circuit).

We measured a white noise of  $15 \mu\phi_0/\sqrt{\text{Hz}}$  in this configuration, corresponding to a field resolution of  $22 \text{ fT}/\sqrt{\text{Hz}}$ . This design still has the disadvantage of not entirely separating the rf and dc circuits. The rf shunt does not carry all of the rf current across the slit. Hence, the multiturn coil damps the coplanar resonator, resulting in a reduced quality factor  $Q$ .

To improve the design, we considered the following points:

- The pickup loop of the dc circuit should enclose the entire substrate area of  $1 \text{ cm}^2$  to minimize  $\partial B/\partial \phi$ .
- The resonator should have a small size, because it must be embedded into the pickup loop, but  $f_0$  should still not exceed the critical frequency  $f_c = R_N/(2\pi L_s)$ .
- The two circuits (rf and dc) should be fully separated.

To meet these requirements, we developed the labyrinth resonator, which is shown together with the layout of the rf SQUID magnetometer in Fig. 9 [48]. For a 5-ring resonator with a diameter of 5.5 mm, we found  $f_0 = 460 \text{ MHz}$  and  $Q_0$  of about 1000. The condition for optimum SQUID operation ( $k^2Q > 1$ ) could be easily fulfilled because of the better coupling between the SQUID and the labyrinth resonator.

The  $\partial B/\partial \phi$  of this layout was found to be lower than  $0.9 \text{ nT}/\phi_0$ . The field resolution of this rf SQUID magnetometer was about  $11.5 \text{ fT}/\sqrt{\text{Hz}}$ , which is comparable to values obtained by the best HTS dc SQUIDs.

The work on the third generation is still at a preliminary stage. The film quality plays a major role for the low frequency noise and now has to be improved even further.